POLITECNICO DI TORINO
Repository ISTITUZIONALE

Amino groups modified SBA-15 for dispersive-solid phase extraction in the analysis of micropollutants by QuEchERS approach

(Article begins on next page)

01 August 2024

1 **Amino groups modified SBA-15 for dispersive-solid phase extraction in the analysis of**
2 **micropollutants by QuEchERS approach**

3

4

5 Michele Castiglioni[a], Barbara Onida[b]*, Luca Rivoira[a], Massimo Del Bubba[c], Silvia Ronchetti[b],
6 Maria Concetta Bruzzoniti[a]*

7

8 [a] Department of Chemistry, University of Turin, Via P. Giuria 7, 10125 Turin, Italy

9 [b] Department of Applied Science and Technology, DISAT, Polytechnic of Turin, Corso Duca degli
10 Abruzzi 24, 10129 Turin, Italy

11 [c] Department of Chemistry "Ugo Schiff", University of Florence, Via della Lastruccia 3, 50019
12 Sesto Fiorentino, Florence, Italy

13

14 ***Corresponding Authors**

15 Prof. Maria Concetta Bruzzoniti

16 ORCID ID 0000-0002-9144-9254

17 Department of Chemistry

18 University of Turin

19 Via P. Giuria 7, 10125 Turin, Italy

20

21 **And**

22

23 Prof. Barbara Onida

24 ORCID ID 0000-0002-1928-3579

25 Department of Applied Science and Technology

26 DISAT, Polytechnic of Turin

27 Corso Duca degli Abruzzi 24, 10129 Turin, Italy

28

Abstract

In the analysis of contaminants in food products, sample preparation is performed by proper adsorbents, whose choice is crucial to eliminate matrix interference. In this work we modified SBA-15 adsorbents by functionalization with (3-aminopropyl)-triethoxysilane (SBA-15-APTES) and N-[3-(trimethoxysilyl)propyl]aniline (SBA-15-AN) aiming to use them for the first time in the clean-up step of a QuEChERS (quick, easy, cheap, effective, rugged and safe) extraction of micropollutants from strawberry, a sugar rich fruit. After physico-chemical characterization by nitrogen adsorption, infrared spectroscopy and thermogravimetric analysis, the adsorption capabilities of SBA-15 sorbents and possible interaction mechanisms were studied at different pH (2.1-8.5) for glucose, sucrose and fructose at concentrations characteristic of those found in strawberries. The performance of the two SBA-15 sorbents was compared with that of commercial PSA (primary secondary amine), usually proposed in QuEChERS protocols. Both SBA-15 materials exhibit up to 30% higher adsorption than PSA, suggesting their possible QuEChERS application. Synthesized SBA-15 adsorbents were hence used as innovative dispersive sorbents in the QuEChERS extractions of 13 PAHs and 14 PCBs from strawberry. For PCBs, SBA-15-AN provides better matrix removal than PSA and comparable extraction recoveries around 90%. For PAHs, the use of SBA-15-AN has the advantage of lower relative standard deviation (7%) than PSA (19%).

1. Introduction

Fruits and their transformation products (e.g. beverages and jams) may be altered by organic micropollutants due to many contamination sources, such as soil and irrigation water [1, 2], as well as packaging materials [3] and pesticide application [4].

Current regulation regarding the presence of organic micropollutants in fruits and vegetables includes polycyclic aromatic hydrocarbons (PAHs), polychlorinated dibenzo(p)dioxins (PCCDs), polychlorinated dibenzo(p)furans (PCDFs), and polychlorinated biphenyls (PCBs) with dioxin-like properties, referred to as dioxine-like PCBs (DL-PCBs) [5].

Most of the above-mentioned compounds in fruits and derived products are analysed by using the QuEChERS approach followed by gas chromatographic-mass spectrometric analysis (GC-MS) [2, 6]. QuEChERS extraction is based on the partition of target analytes between water and acetonitrile.

2

62   Sugars present as natural components or as additives are well-known interferents in the

63   QuEChERS approach since they are co-extracted in acetonitrile and must be removed prior to the

64   analysis of the extracted samples by chromatographic methods.

65   This task is usually accomplished using solid-phase extraction (SPE) cleanup, even through

66   on-line approaches [7], or by a dispersive solid phase extraction (*d*-SPE) clean-up step, with a primary

67   secondary amine (PSA) sorbent [8, 9]. Several manufacturers make commercially available

68   proprietary PSA sorbents which are based on silica chemically modified with ethylenediamine-N-

69   propyl group, as bulk packing, or within ready-to-use kits for QuEChERS analysis. PSA is usually

70   claimed to be a sorbent more retentive than aminopropyl phases due to presence of the secondary

71   amine [10], even if dedicated studies on the adsorption mechanisms are not yet available.

72   Ordered mesoporous silicas and organosilicas have been largely investigated as adsorbents

73   [11-14] due to their high specific surface area and uniform porosity, together with the possibility of

74   tailoring their surface chemical properties through synthesis conditions and post-synthesis

75   modification. In particular, in the context of analytical chemistry, ordered mesoporous organosilicas

76   have been tested as adsorbents for food samples cleanup [15].

77   Mesoporous silica functionalized with amino groups was previously investigated for

78   adsorption and removal of anionic pollutants in wastewater [16, 17].

79   The aim of this work is to synthesize and study the performance of organically modified

80   ordered mesoporous silicas to be innovatively included as *d*-SPE sorbents in a QuEChERS protocol

81   for the removal of co-extracted sugars for the analysis of contamination of strawberries by 13 PAHs

82   and 14 PCBs, including dioxine-like congeners. PCBs and PAHs are often found in fruit [18, 19] and

83   are therefore a major concern for health protection.

84   Ordered mesoporous silica of SBA-15 family was functionalized with the primary amine (3-

85   aminopropyl)-triethoxysilane (APTES) and, in another case, with the secondary amine N-[3-

86   (Trimethoxysilyl)propyl]aniline, in order to mimic the commercial PSA. After the determination of

87   the main physico-chemical characteristics, the adsorption of glucose, fructose and sucrose (sugars

88   naturally contained in fruit) was studied. The performances of the two organically modified SBA-15

89   silica as QuEChERS d-SPE sorbents were investigated determining the signal to noise ratio and the

90   extraction recoveries for target compounds, in comparison with those obtained by commercial PSA.

91   To the best of our knowledge no reports are currently available on the use of ordered

92   mesoporous organosilicas in the QuEChERS technique.

93

94   **2. Materials and Methods**

95   *2.1 Reagents*

3

All reagents used were of analytical grade. Ordered mesoporous silica of the SBA-15 type was purchased from ACS Material Advanced Chemical Supplier (Pasadena, CA, USA). (3-aminopropyl) triethoxysilane (APTES, 99%), N-[3-(Trimethoxysilyl)propyl]aniline, toluene (99.8%), acetonitrile (>99.9%) were purchased from Sigma Aldrich (Steinheim, DE). Primary Secondary Amine (PSA, Figure 1A) was purchased from Agilent Technologies (Santa Clara, CA, USA). D(+) glucose was purchased from Merck (Darmstadt, DE), D(-) fructose and sucrose were purchased from J.T. Baker (Phillipsburg, NJ, USA).

The PAHs studied were the 13 PAH compounds listed by EPA 525.1 procedure and were purchased from Sigma Aldrich-Merck (Darmstadt, Germany): acenaphtylene (AcPY), fluorene (Flu), phenanthrene (Phe), anthracene (Ant), pyrene (Pyr), benzo[a]anthracene (BaA), chrysene (Chr), benzo[b]fluoranthene (BbFl), benzo[k]fluoranthene (BkFl), benzo[a]pyrene (BaP), indeno[1,2,3-cd]pyrene (Ind), dibenzo[a,h]anthracene (DBA), benzo[ghi]perylene (BP). PCBs were purchased from LGC Standards (Milan, Italy). They were non-dioxine like PCBs: 3,3'-dichlorobiphenyl (PCB 11), 4,4'-dichlorobiphenyl (PCB 15), 2,4,4'-trichlorobiphenyl (PCB 28), 2,2',5,5'-tetrachlorobiphenyl (PCB 52), 2,2',4,5,5'-pentachlorobiphenyl (PCB 101), 2,2',3,4,4',5-hexachlorobiphenyl (PCB 138), 2,2',4,4',5,5'-hexachlorobiphenyl (PCB 153), 3,3',4,4',5,5'-hexachlorobiphenyl (PCB 169), 2,2',3,4,4',5,5'-heptachlorobiphenyl (PCB 180), 2,3,3',4,4',5,5'-heptachlorobiphenyl (PCB 189); and dioxine like PCBs: 3,4,4',5-tetrachlorobiphenyl (PCB 81), 2,3',4,4',5-pentachlorobiphenyl (PCB 118), 2',3,4,4',5-pentachlorobiphenyl (PCB 123), 2,3',4,4',5,5'-hexachlorobiphenyl (PCB 167).

Hydrochloric acid (35% w/w, d = 1.187 g/mL) and NaOH (>98%) were from Carlo Erba (Milano, IT). NaCl, $MgSO_4 \cdot 7H_2O$ and H_2SO_4 (95–97%, d = 1.84 g/mL) were from Sigma-Aldrich. High-purity water (18.2 M Ω·cm resistivity at 25°C), produced by an Elix-Milli Q Academic system from Millipore (Vimodrone, MI, Italy) was used for standard and eluent preparation.

2.2 Preparation of sorbents

The synthesis procedures of the two sorbents were based on previous work concerning on the functionalization of SBA-15 silica [16, 17]. In a flask, 1 g of SBA-15, previously washed with about 50 mL of deionized water, was stirred with 200 mL of toluene for 30 min, at room temperature. Afterwards, 2 mL of functionalizing reagent ((3-aminopropyl)-triethoxysilane-APTES or N-[3-(trimethoxysilyl)propyl]aniline, Fig. 1B and 1C) was added dropwise. The flask was then connected to a water-refrigerated system and the solution heated to 110 ° C. The solution was kept under stirring for 24 hours. Afterwards, the powder was filtered and dried.

4

Hereafter the sample functionalized with APTES is denoted SBA-15-APTES and the sample functionalized with N-[3-(trimethoxysilyl)propyl]aniline is denoted SBA-15-AN.

2.3 Physico-chemical characterization

Nitrogen adsorption isotherms were measured using a Quantachrome AUTOSORB-1 (Boynton Beach, FL, USA) instrument. Prior to nitrogen adsorption, samples were outgassed at 393 K for 6 h. The BET specific surface areas (SSA) were calculated in the relative pressure range from 0.04 to 0.1 and the pore size distribution were determined through the NLDFT (Non Localized Density Functional Theory) method, using the equilibrium model for cylindrical pores.

For FTIR measurements, powders were pressed in self-supporting wafers and spectra were recorded at room temperature with a Bruker Tensor 27 (Bruker, Billerica, MA, USA) spectrometer operating at 2 cm^{-1} resolution, after outgassing the sample at room temperature (residual pressure of 0.1 Pa).

TG analyses were carried out between 298 K and 1073 K in air (flow rate 100 mL/min with a heating rate of 10 K/min) using a SETARAM 92 (Caluire, France) instrument.

Density functional theory (DFT) simulations were calculated by means of Gaussian 09W and Gaussian View (Gaussian Inc, Wallington, US).

2.4 Chromatographic analysis

The evaluation of sugar content was performed by ion-chromatography using an ICS-3000 gradient pump, Thermo Fisher Scientific, Waltham, MA, USA, coupled to pulsed amperometric detection. An AD40 Electrochemical Detector, Thermo Fisher Scientific, equipped with Ag/AgCl reference electrode and a gold working electrode was used. The detection potential was set at 0.1 V and maintained for 400 ms: the first 200 ms represents the delay time and the second 200 ms represents the determination time. The potential was then instantaneously set at -2 V and maintained for 10 ms and raised at 0.6 V and maintained for 10 ms to restore the gold oxide necessary to maintain an active working electrode surface. The potential was finally set at -0.1V and maintained for 60 ms, to reduce the small amount of gold oxide previously formed. The waveform requires a total of 500 ms.

The sample (10 µL) was injected through a six-ways Rheodyne injection valve. The column used was a CarboPacPA10, 250x4 mm (100 µeq/column), Thermo Fisher Scientific which has a microporous substrate with particle size of 10 µm, 55% cross-linking functionalized with a difunctional quaternary ion latex (5% cross-linking).

162   After optimization, the eluent concentration was kept at 55 mM KOH (data available upon

163 request). At these conditions, limits of detection (LODs) for glucose, fructose and sucrose, calculated

164 as $s_m=s_m+3s_b$, with s_m=average signal of blank, s_b= standard deviation of blank on ten measurements,

165 were respectively 69, 56 and 11 µg/L. Pump, detector settings, and data collection were managed by

166 the Chromeleon v.6.80 software (Thermo Fisher Scientific).

167   For PAHs and PCBs analysis, a gas chromatographic-mass spectrometric (GC-MS) method

168 was used, according to previous studies by our research group [2, 20], employing an Agilent (Santa

169 Clara, CA,USA) 6980 series gas chromatograph coupled with an Agilent 5973 Network mass

170 spectrometer detector.

171   The GC column was a (5%-Phenyl)-methylpolysiloxane column (HP 5ms, 30 m x 0.25 mm x

172 25 µm, Agilent), with He as gas carrier (1 mL/min). MS detection was performed in Single Ion

173 Monitoring (SIM) mode, selecting for each analyte its proper m/z ratio (m/z ratio available upon

174 request). 2 µL of each sample were injected using the Pulsed Splitless mode (pressure at 40 psi for

175 2.5 min). The oven ramp was: 90°C, hold for 2 min; ramp to 176 °C, 12 °C/min rate; ramp to 196°C,

176 5 °C/min rate, hold for 3 mins; ramp to 224°C, 12 °C/min rate; ramp to 244 °C, 5°C/min rate, hold

177 for 3 min; ramp to 270 °C, 7°C/min rate, hold for 3 min; ramp to 300 °C, 5°C/min, hold for 10 min

178 to completely clean and restore the GC column. The total run time for the complete separation of

179 PAHs and PCBs is 52 min.

180   LODs, calculated as previously described for ion chromatography, were in the range from

181 0.06 µg/L (BaA) to 2.10 µg/L (DBA), while from 0.49 µg/L (PCB153) to 5.40 µg/L (PCB169).

182 Detailed analytical features of the GC-MS method are presented in Table S1 (for PAHs) and S2 (for

183 PCBs) of the Supplementary Information section.

184   GC-MS data were handled with OpenChrome software (Lablicate, Germany).

185

186   *2.5 Adsorption tests*

187   Tests to evaluate the effect of pH were performed on 0.25 g of sorbent. The sorbent was put

188 in contact with 4 g solution containing 350 mg/g glucose, 350 mg/g fructose and 170 mg/g sucrose.

189 These concentrations were chosen in order to match those contained in strawberry according to

190 Kasperbauer [21]. Solutions were stirred at 1100 xg for 10 min. Experiments were performed at pH

191 2.1, 5.0 and 8.5.

192

193   *2.6 Strawberry fruits*

194   Commercial strawberry samples grown in Italy were used. *Fragaria x ananassa, Camarosa*

195 cultivar was chosen as model plant, since it accounts for about 60% of the strawberry world's

196 production and it adapts greatly to wide climate and growth conditions.

197

198   *2.7 Extraction of PAHs and PCBs from strawberries by QuEChERS*

199   Among organic micropollutants, PCBs and PAHs, present in the environment as a result of

200 natural and anthropogenic processes, represent both point source and diffuse emissions [22].

201   PAHs and PCBs were extracted using a QuEChERS approach [8, 23]. Briefly, 5 g of

202 homogenized strawberries were put in a vial containing 10 mL acetonitrile:H_2O pH 2.1 (70:30), 8.2

203 g $MgSO_4$ and 1 g NaCl. The tube was vigorously shaken and centrifuged at 1100 xg for 10 min. After

204 extraction, a 4 mL aliquot of the supernatant was then transferred in a new vial containing 0.25 g of

205 sorbent (PSA or SBA-15-APTES or SBA-15-AN) and 1.0 g $MgSO_4$ for the clean-up step. The tube

206 was shaken and centrifuged (7870 xg, 10 min) and the supernatant was directly analysed by GC-MS.

207 For each sorbent, the recovery was calculated spiking the fruit samples prior- (i) and post- (ii)

208 extraction as follows:

209   • Pre-extraction spike: a cumulative batch of 50 g of homogenised strawberries was spiked with

210   6666 µL of a solution containing PAHs and PCBs at 300 µg/L each, to achieve a final

211   concentration of 0.04 mg/kg. According to the extraction procedure above detailed, a

212   theoretical final concentration of 20 µg/L is expected for each PAH and PCBs. The procedure

213   was repeated in triplicate.

214   • Post-extraction spike: after the extraction and clean-up procedure, 187 µL of the extract is

215   spiked with 13 µL of the solution containing PAHs and PCBs at 300 µg/L, so to obtain a final

216   concentration of 20 µg/L for each PAH and PCBs. The procedure was repeated in triplicate.

217

218   For each analyte, extraction recovery percentage (ER%) was calculated from the peak areas

219 obtained after the pre-extraction spike ($A_{pre-extraction}$) and post-extraction ($A_{post-extraction}$) according to

220 the equation:

221    $ER\% = 100 * A_{pre-extraction} / A_{post-extraction}$

222

223   For each analyte and experimental conditions, signal-to-noise ratio (S/N) was derived from

224 the software OpenChrome and was calculated from the height of the analyte chromatographic peak

225 (H_{peak}) and that of the noise (h_{noise}), according to the 2015 United States Pharmacopeia definition [24]:

226    $S/N = 2H_{peak}/h_{noise}$

227

3. Results and discussion

3.1 Physico-chemical characterization

Table 1 reports textural features of SBA-15 as such and of functionalized SBA-15. For both SBA-15-APTES and SBA-15-AN, lower values of SSA, pore volume and pore diameter are observed with respect to the pristine SBA-15. These results reveal that grafting of organic moieties on the internal surface of silica mesopores occurred during functionalization.

N_2 adsorption measurement was carried out also on PSA since no data for the commercial product were available. It is worth noting that the same features of PSA are in between those of SBA-15 and organically modified SBA-15, so that, as a whole, we can consider PSA, SBA-15-APTES and SBA-15-AN comparable systems for the proposed QuEChERS application.

Fig. 2 shows FT-IR spectra of SBA-15, SBA-15-APTES and SBA-15-AN after outgassing at room temperature.

The spectrum of SBA-15 (curve 1) reveals the typical features of an amorphous silica, i. e. the narrow band at 3743 cm^{-1}, due to the stretching mode of isolated silanols, and the broad band centred at 3530 cm^{-1}, due to H-bonded silanols.

In the spectrum of SBA-15-APTES (curve 2), bands due to the organic moieties are clearly observed, that are: i) two bands at 3355 cm^{-1} and 3295 cm^{-1} attributed to the stretching modes of -NH_2 groups; ii) two bands at 2930 cm^{-1} and 2875 cm^{-1} due to the stretching modes of aliphatic -CH_2- groups; iii) a band at about 1595 cm^{-1} due to the bending mode of -NH_2 groups. As usually observed for amorphous silica modified with APTES, a broad and ill-defined absorption is observed at about 3000 cm^{-1}, on which the previous mentioned bands are superimposed. This absorption is due to the residual silanols engaged in H-bonding with surface -NH_2 groups [25]. Indeed, in the spectrum, the stretching mode of isolated silanols is not present.

In the case of SBA-15-AN (curve 3), as for SBA-15-APTES, the bands due to the organic groups are visible in the spectrum, i.e. i) the band at 3330 cm^{-1} due to the stretching mode of -NH- species; ii) bands above and below 3000 cm^{-1} due to, respectively, aromatic -CH and aliphatic -CH_2- stretching modes; iii) bands below 1700 cm^{-1} due to ring modes of the aromatic moieties. Moreover, a broad absorption is observed at about 3600 cm^{-1} which is tentatively ascribed to the residual silanols engaged in H-bonding with aromatic rings [26].

In summary, the set of IR data reveal that amine species in modified SBA-15 are located and exposed on the silica surface, in agreement with textural features (Table 1) discussed above.

From TG curves (not reported), the amount of amino groups was estimated and it is 4.41 mmol/g for SBA-15-APTES and 2.23 mmol/g for SBA-15-AN.

8

According to data found for commercially available PSA in the market, capacity for PSA ranges from 0.65 to 1.22 mmol/g [27, 28]. The above-mentioned capacity data suggest, per se, a competitive performance of functionalized SBA-15 in respect to PSA, and supports the study herein proposed.

3.2 Adsorption measurements

The following experiments were performed in order to optimize the pH conditions to be used in QuEChERS application. Furthermore, the results may be useful in formulating possible interactions acting between adsorbents and sugars during retention.

Results are represented in Fig. 3A, 3B, 3C. According to the acidic dissociation constants of the sugars considered (pK_a=12.2 for glucose, 12.0 for fructose and 12.6 for sucrose), the concentration of dissociated sugars may be considered negligible at pH values studied (2.1, 5.0 and 8.5).

Organically modified mesoporous silicas show better removal performance than commercial PSA for all the pH values. It is worth noting that textural properties such as SSA and pore volume of SBA-15-APTES and SBA-15-AN are comparable to those of PSA (see Table 1), therefore the better adsorption performance of organically modified mesoporous silica has to be ascribed to the functional groups acting as adsorption sites, the amount of which is larger in SBA-15-APTES and SBA-15-AN than in PSA. Nevertheless, a role of different surface chemical properties of the two silica supports, cannot be ruled out.

Firstly, the retention properties of aminopropyl-modified silica and PSA towards sugars has been ascribed mainly to H-bonding [29]. The role of H-bonding of protonated ethylenediamine based materials, structurally similar to PSA, in the retention of uncharged compounds is supported by many authors [30, 31], who also speculated on possible leading retention mechanisms via H-bonding as a function of pH and on the abundancy of NH_3^+/NH_2 and NH_3^+/NH groups [31].

As shown in Fig. 3, for all the adsorbents, retention capabilities decrease at increasing pH. This may be ascribed to a change of the relative population of protonated and deprotonated amine groups and to their involvement in H-bonding. At increasing pH, the population of protonated amines decreases. Since protonated amines are stronger Brønsted acids than amines, they may be considered also stronger H donor in H-bonding.

Data in Fig. 3A-3B-3C show that SBA-15-AN has higher retention abilities than SBA-15-APTES at all the pH values tested (SBA-15-AN > SBA-15-APTES > PSA). Indeed, if we consider that aniline (pK_b 8.9) is a weaker base than propylamine (pK_b 3.5), the decrease of protonated amine population upon increasing pH is expected to be relatively larger in SBA-15-AN than SBA-15-APTES. Thus, it may be proposed that H-bonding between protonated amines and sugar molecules,

9

where the former act as proton donor and the latter as proton acceptor, does not play the only role in the adsorption.

Therefore, the better performance of SBA-15-AN compared to that of SBA-15-APTES can be ascribed to a higher hydrophobicity of the material due to the more hydrophobic functional group, which is usually desired in case of organic molecules adsorption from water solution. Moreover, the electron-withdrawing effect of the aromatic ring enhances the positive charge of the ammonium group, increasing the strength of H-bonding with sugar molecules.

Experimental tests indicated that pH 2.1 is the optimal pH value to achieve the highest sugars adsorption in a QuEChERS application.

3.3 Organically modified mesoporous silicas in the d-SPE cleanup of QuEChERS

In a QuEChERS procedure, after extraction with acetonitrile, a clean-up step performed in *d*-SPE is necessary to remove coextracted interferents without losing analytes of interest.

To this purpose, the capabilities of SBA-15-APTES and SBA-15-AN as *d*-SPE sorbents were investigated in the determination of persistent pollutants (PAHs and PCBs, included dioxine-like congeners) in strawberries, using the QuEChERS extraction approach.

Performances of the modified silicas were studied and compared with those of PSA, measuring both signal-to-noise ratio (S/N) and extraction recovery (ER) of PAHs and PCBs after the application of the QuEChERS protocol.

S/N is a parameter characteristic of the chromatogram and indicates the quantification accuracy of the components during the analytical separation. The higher the S/N, the better recognized the analyte and the lower the detection limits obtainable. Due to this intrinsic property, S/N is considered a primary standard for comparison of chromatographic performances [32] and it is therefore frequently used as response in analytical design optimizations [32-34]. In a complex matrix, such as strawberry rich in sugars, anthocyanins and polyphenols [35], S/N is indicative of the efficiency of matrix removal.

Additionally, ER was also measured, since it is indicative of the efficiency of the whole method (extraction and cleanup) to extract analytes of interest, without losing them by adsorption during the clean-up step.

Results obtained by our study for S/N are reported in Fig. 4 (PAHs) and 5 (PCBs) while ER values are shown in Fig. 6 (PAHs) and 7 (PCBs). Data obtained in the absence of the *d*-SPE treatment were also considered.

For an easier interpretation, for each sorbent, experimental results for PAHs are shown, in Fig. 4 and 6, as single value or as average for compounds: up to four benzene rings (acenaphtylene, the

10

330 isomers: phenanthrene/anthracene; fluorene/pyrene; benzo[a]anthracene/chrysene);

331 four benzene rings around a 5-membered ring and five benzene rings (the isomers:

332 benzo[b]fluoranthene/benzo[k]fluoranthene/benzo[a]pyrene); five benzene rings or five benzene

333 rings around a 5-membered ring (dibenzo[a,h]anthracene and the isomers indeno[1,2,3-

334 cd]pyrene/benzo[ghi]perylene). For PCBs, for each sorbent, experimental results were shown, in Fig.

335 5 and 7, as single value or as average for the 14 congeners tested.

336 As regards S/N values, for all the analytes (Fig. 4 and 5), the values obtained without a *d*-SPE

337 treatment are the lowest, indicating a poor quality of the analytical method. The increase of S/N values

338 in the presence of the *d*-SPE treatment indicates a better detectability, essentially due to the removal

339 of coextracted matrix compounds, and the consequent improvement of the baseline. In this regard,

340 both the organically modified mesoporous silica are effective in improving the analytical method.

341 For PAHs (Fig. 4), S/N obtained with PSA are higher than those obtained with SBA-15-

342 APTES and SBA-15-AN for all the hydrocarbons, except for the last three heaviest compounds for

343 which SBA-15-AN is the best performing d-SPE sorbent. The improvement of S/N for these last

344 compounds (about 30%) turns to be important in the enhancement of the detection limits in real

345 matrices, since the heaviest compounds are affected by poor detectability.

346 For PCBs (Fig. 5), the highest S/N is observed for SBA-15-AN, for which, on average, an

347 improvement of S/N values of about 20% in respect to PSA is observed.

348 Extraction recovery ER% as a function of the d-SPE sorbent used is shown in Fig. 6 for PAHs

349 and in Fig. 7 for PCBs.

350 For the 13 PAHs, average ER% follows the order PSA (76±19 %) > SBA-15-AN (63±7 %) >

351 SBA-15-APTES (61±14 %), even though comparable performances are observed for PSA and SBA-

352 15-AN for lower molecular weight PAHs. Differently, ER% obtained without any d-SPE sorbent are

353 significantly lower, ranging from 14±3 to 25±2% (data not shown).

354 According to the Anova test (p=0.0001, 95% confidence interval), the average ER for PSA is

355 statistically different from SBA-15-AN and SBA-15-APTES, whereas average ER for the two

356 organically modified mesoporous silica do not show statistical difference. Despite the higher ER

357 obtained for PSA, the lower standard deviation observed for SBA-15-AN indicates that the d-SPE

358 cleanup with SBA-15-AN is more reliable than the one performed with PSA. Statistic variability of

359 ER% values for each sorbent was also evaluated through Horwtiz equation (Thompson modification

360 [36]), calculating at first the concentration of each PAH, according to its extraction yields, and finally

361 the maximum acceptable RSD%. Since the maximum acceptable RSD% value calculated was 22%,

362 the average RSD% values observed for PAHs with each sorbent (26.2% for PSA and 14.2% for SBA-

363 15-AN) indicate that the use of PSA provided recoveries falling outside the range of acceptability.

11

364 Differently, the reliability of SBA-15-AN is confirmed since average RSD% is far below the Horwitz

365 value.

366   Data shows that for all the *d*-SPE sorbents, a decrease of ER% is observed with the increase

367 of molecular weight introduced by the aromatic rings. This behaviour was verified for PSA also by

368 Sadowska-Rociek et al [37] in the analysis of PAHs in tea.

369   Even if, overall, PSA is the best performing sorbent for all PAHs, SBA-15-APTES provides

370 higher ER% for higher molecular weight PAHs.

371   For PCBs, average ER% follows the order PSA (92±6 %) > SBA-15-AN (88±9 %) > SBA-

372 15-APTES (67±17 %). Again, poor recovery is observed without any d-SPE step (ER% ranging from

373 36±6 to 44±7%, data not shown). The average ER values obtained for PSA and SBA-15-AN are not

374 statistically different (Anova test, p=0.0001, 95% confidence interval), whereas average ER values

375 obtained with SBA-15-APTES statistically differ from those obtained by PSA and SBA-15-AN.

376 Again, the application of the Horwitz equation (calculated RSD%=22%), confirmed the statistical

377 acceptability for recoveries obtained with PSA and SBA-15-AN (RSD%=7.2% and 10.2%,

378 respectively), but not with SBA-15-APTES (RSD%=25.8%).

379   Presuming that the extraction recovery calculation used compensates for any matrix effect, it

380 is reasonable to assume that differences in extraction recovery values observed among the three d-

381 SPE materials is due to the different extent of adsorption of PAHs and PCBs by each sorbent, being

382 the extraction procedure the same for the three tests.

383   For each sorbent, PCBs exhibit higher ER% values than PAHs. For each d-SPE sorbent, for

384 PAHs an increase of ER% is observed upon decreasing molecular weight (MW), showing a partial

385 anticorrelation (the higher the MW, the lower the ER%) for SBA-15-AN (ER% = -1.9 MW + 346,

386 r^2= 0.919) and for SBA-15-APTES (ER% = -3.3 MW + 424, r^2= 0.840), while for PSA this behaviour

387 is not well evidenced (ER% = -1.5 MW + 340, r^2= 0.429). This suggests that at variance with what

388 hypothesized by Dachs and Bayona [38] for silica based octadecyl substrates, in this case, steric

389 hindrance and shape selectivity do not play a crucial role in the extraction. To explain the higher

390 extent of adsorption observed for higher molecular weight PAHs, density functional theory (DFT)

391 simulations were calculated by the software Gaussview 6.0 in order to estimate the potential and

392 charge density distribution for each PAH tested [39].

393   Results obtained (Fig.8) show that the centre of each ring on both sides of the PAH molecular

394 plane is negatively charged and corresponds with delocalized π electrons. Indeed, the area of the π-

395 electron plane spatially increases when the number of rings increased, as demonstrated also by Yang

396 and co-workers [40]. Hence, the heavier molecular weight of the PAHs offers higher surface

397 availability for interaction with positively charged amino groups. Moreover, such behaviour is also

12

in agreement with stronger Van der Waals interactions. Conversely, for PCBs, the addition of chlorine atoms on the biphenyl structure enhances steric hindrance, in agreement with observations of Dachs and Bayona [38]. In Fig. 9, as an example, the different behaviour of PAHs (Fig. 9A) and PCBs (Fig. 9B) is compared for SBA-15-AN.

Eventually the polarity of micropollutants was also considered. Variations in logP does not significantly influence the extraction performance of the QuEChERS method when SBA-15-APTES or SBA-15-AN are used as d-SPE sorbents. Instead, an apparent correlation of ER% with log P for both PAHs and PCBs classes is observed only for PSA (ER% = 10.36 logP + 0.49, r^2=0.653), highlighting possible limitations in its use of this d-SPE sorbent for more polar analytes. This observation agrees with what found by Scordo et al. [1] in the extraction of perfluoroalkyl acids from strawberry.

4. Conclusions

SBA-15 mesoporous silica were functionalized with (3-aminopropyl)-triethoxysilane (SBA-15-APTES) and N-[3-(Trimethoxysilyl)propyl]aniline (SBA-15-AN) and used for the first time as d-SPE sorbents in the removal of coextracted compounds (e.g. sugars) in the QuEChERS protocol applied for the determination of micropollutants (PAHs and PCBs) in strawberry. SBA-15-APTES and SBA-15-AN were physico-chemically characterized and compared with PSA, the d-SPE sorbent usually employed in QuEChERS application. The removal capabilities of SBA-15-APTES and SBA-15-AN towards glucose, sucrose and fructose, chosen as model sugars present in strawberry was observed to be higher than that of PSA, due to the higher amount of adsorption active sites. A thorough study of the effect of pH on removal of sugars allowed to propose an interaction mechanism between amines and sugar molecules mainly based on H-bonding.

The suitability of SBA-15-APTES and SBA-15-AN as *d*-SPE sorbents were confirmed including these sorbents in the clean-up step of a QuEChERS protocol for the determination of PAHs and PCBs in intentionally contaminated strawberries. Signal-to-noise ratio for PCBs can be significantly reduced by SBA-15-AN, indicating even a more efficient cleanup if compared to PSA. It is worth remembering that the reduction of signal-to-noise ratio is important to determine lower concentrations of micropollutants in food. Overall, QuEChERS protocol performed by SBA-15-AN provides slightly lower or comparable extraction recoveries than PSA (63±7 % vs 76±19 % for PAHs, respectively and 92±6 % vs 88±9 % for PCBs) and better reproducibility of the method. Molecular weight of the target micropollutants, but not log P, seem to influence the overall QuEChERS extraction recovery in the organically modified SBA-15.

Declaration of Competing Interest

The authors declare that they have no known competing financial interests or personal relationships that could have appeared to influence the work reported in this paper.

Supplementary Information

The manuscript contains supplementary material.

CRediT author statement

M. Castiglioni: investigation, writing original draft, manuscript revision. **B. Onida:** data interpretation, review and manuscript editing. **L. Rivoira:** supervision, data validation and curation, manuscript revision. **M. Del Bubba:** data interpretation, manuscript editing. **S. Ronchetti:** data interpretation, review. **M.C. Bruzzoniti:** conceptualization, data interpretation, review and manuscript editing, funding acquisition, manuscript revision.

References

[1] C.V.A. Scordo, L. Checchini, L. Renai, S. Orlandini, M.C. Bruzzoniti, D. Fibbi, L. Mandi, N. Ouazzani, M. Del Bubba, Optimization and validation of a method based on QuEChERS extraction and liquid chromatographic–tandem mass spectrometric analysis for the determination of perfluoroalkyl acids in strawberry and olive fruits, as model crops with different matrix characteristics, J. Chromatogr. A 1621 (2020) 461038. https://doi.org/https://doi.org/10.1016/j.chroma.2020.461038.
[2] L. Rivoira, M. Castiglioni, A. Kettab, N. Ouazzani, E. Al-Karablieh, N. Boujelben, D. Fibbi, E. Coppini, E. Giordani, M.D. Bubba, M.C. Bruzzoniti, Impact of effluents from wastewater treatments reused for irrigation: Strawberry as case study, Environmental Engineering and Management Journal 18(10) (2019) 2133-2143.
[3] K. Grob, M. Biedermann, E. Scherbaum, M. Roth, K. Rieger, Food contamination with organic materials in perspective: packaging materials as the largest and least controlled source? A view focusing on the European situation, Critical reviews in food science and nutrition 46(7) (2006) 529-535. https://doi.org/10.1080/10408390500295490.
[4] L. Sung-Jin, O. Young-Tak, J. You-Sung, R. Jin-Ho, C. Geun-Hyoung, Y. Ji-Yeon, P. Byung-Jun, Persistent organic pollutants (POPs) residues in greenhouse soil and strawberry organochlorine pesticides, Korean Journal of Environmental Agriculture 35(1) (2016) 6-14. https://doi.org/https://doi.org/10.5338/KJEA.2016.35.1.05.
[5] European Commission, 2014/663/EU: Commission Recommendation of 11 September 2014 amending the Annex to Recommendation 2013/711/EU on the reduction of the presence of dioxins, furans and PCBs in feed and food Text with EEA relevance, (2014).

472   [6] M. Anastassiades, S.J. Lehotay, D. Stajnbaher, F.J. Schenck, Fast and easy multiresidue method
473   employing acetonitrile extraction/partitioning and "dispersive solid-phase extraction" for the determination
474   of pesticide residues in produce, J. AOAC Int. 86(2) (2003) 412-31.
475   https://doi.org/https://doi.org/10.1093/jaoac/86.2.412.
476   [7] D. Rossini, L. Ciofi, C. Ancillotti, L. Checchini, M.C. Bruzzoniti, L. Rivoira, D. Fibbi, S. Orlandini, M. Del
477   Bubba, Innovative combination of QuEChERS extraction with on-line solid-phase extract purification and
478   pre-concentration, followed by liquid chromatography-tandem mass spectrometry for the determination of
479   non-steroidal anti-inflammatory drugs and their metabolites in sewage sludge, Anal. Chim. Acta 935 (2016)
480   269-281. https://doi.org/10.1016/j.aca.2016.06.023.
481   [8] M.C. Bruzzoniti, L. Checchini, R.M. De Carlo, S. Orlandini, L. Rivoira, M. Del Bubba, QuEChERS sample
482   preparation for the determination of pesticides and other organic residues in environmental matrices: a
483   critical review, Anal Bioanal Chem 406(17) (2014) 4089-4116. https://doi.org/10.1007/s00216-014-7798-4.
484   [9] D. Oshita, I.C.S.F. Jardim, Comparison of Different Sorbents in the QuEChERS Method for the
485   Determination of Pesticide Residues in Strawberries by LC–MS/MS, Chromatographia 77(19) (2014) 1291-
486   1298. https://doi.org/10.1007/s10337-014-2726-5.
487   [10] Y. He, Y.-H. Liu, Assessment of primary and secondary amine adsorbents and elution solvents with or
488   without graphitized carbon for the SPE clean-up of food extracts in pesticide residue analysis,
489   Chromatographia 65(9-10) (2007) 581-590. https://doi.org/https://doi.org/10.1365/s10337-007-0198-6.
490   [11] Z. Wu, D. Zhao, Ordered mesoporous materials as adsorbents, Chem. Commun. 47(12) (2011) 3332-
491   3338. https://doi.org/10.1039/C0CC04909C.
492   [12] C.M. Li, X.P. Wang, Z.H. Jiao, Y.S. Zhang, X.B. Yin, X.M. Cui, Y.Z. Wei, Functionalized Porous Silica-Based
493   Nano/Micro Particles for Environmental Remediation of Hazard Ions, Nanomaterials 9(2) (2019) 247.
494   https://doi.org/https://doi.org/10.3390/nano9020247.
495   [13] P. Kumar, V.V. Guliants, Periodic mesoporous organic–inorganic hybrid materials: applications in
496   membrane separations and adsorption, Microporous Mesoporous Mater. 132(1-2) (2010) 1-14.
497   https://doi.org/https://doi.org/10.1016/j.micromeso.2010.02.007.
498   [14] M.C. Bruzzoniti, E. Mentasti, C. Sarzanini, B. Onida, B. Bonelli, E. Garrone, Retention properties of
499   mesoporous silica-based materials, Anal. Chim. Acta 422(2) (2000) 231-238.
500   https://doi.org/10.1016/S0003-2670(00)01070-9.
501   [15] N. Casado, D. Pérez-Quintanilla, S. Morante-Zarcero, I. Sierra, Current development and applications of
502   ordered mesoporous silicas and other sol–gel silica-based materials in food sample preparation for
503   xenobiotics analysis, TrAC, Trends Anal. Chem. 88 (2017) 167-184.
504   https://doi.org/https://doi.org/10.1016/j.trac.2017.01.001.
505   [16] S. Fiorilli, L. Rivoira, G. Calì, M. Appendini, M.C. Bruzzoniti, M. Coïsson, B. Onida, Iron oxide inside SBA-
506   15 modified with amino groups as reusable adsorbent for highly efficient removal of glyphosate from
507   water, Appl. Surf. Sci. 411 (2017) 457-465. https://doi.org/10.1016/j.apsusc.2017.03.206.
508   [17] L. Rivoira, M. Appendini, S. Fiorilli, B. Onida, M. Del Bubba, M.C. Bruzzoniti, Functionalized iron
509   oxide/SBA-15 sorbent: investigation of adsorption performance towards glyphosate herbicide,
510   Environmental Science and Pollution Research 23(21) (2016) 21682-21691.
511   https://doi.org/10.1007/s11356-016-7384-8.
512   [18] A. Paris, J. Ledauphin, P. Poinot, J.-L. Gaillard, Polycyclic aromatic hydrocarbons in fruits and
513   vegetables: Origin, analysis, and occurrence, Environ. Pollut. 234 (2018) 96-106.
514   https://doi.org/https://doi.org/10.1016/j.envpol.2017.11.028.
515   [19] A.A. Lovett, C.D. Foxall, C.S. Creaser, D. Chewe, PCB and PCDD/DF congeners in locally grown fruit and
516   vegetable samples in Wales and England, Chemosphere 34(5) (1997) 1421-1436.
517   https://doi.org/https://doi.org/10.1016/S0045-6535(97)00439-6.
518   [20] M.C. Bruzzoniti, L. Rivoira, M. Castiglioni, A. El Ghadraoui, A. Ahmali, T. El Hakim El Mansour, L. Mandi,
519   N. Ouazzani, M. Del Bubba, Extraction of polycyclic aromatic hydrocarbons and polychlorinated biphenyls
520   from urban and olive mill wastewaters intended for reuse in agricultural irrigation, J. AOAC Int. 103(2)
521   (2020) 382-391. https://doi.org/10.5740/jaoacint.19-0257.

522 [21] M.J. Kasperbauer, J.H. Loughrin, S.Y. Wang, Light Reflected from Red Mulch to Ripening Strawberries
523 Affects Aroma, Sugar and Organic Acid Concentrations, Photochem. Photobiol. 74(1) (2001) 103-107.
524 https://doi.org/https://doi.org/10.1562/0031-8655(2001)0740103LRFRMT2.0.CO2.
525 [22] C.H. Vane, A.W. Kim, D.J. Beriro, M.R. Cave, K. Knights, V. Moss-Hayes, P.C. Nathanail, Polycyclic
526 aromatic hydrocarbons (PAH) and polychlorinated biphenyls (PCB) in urban soils of Greater London, UK,
527 Appl. Geochem. 51 (2014) 303-314. https://doi.org/https://doi.org/10.1016/j.apgeochem.2014.09.013.
528 [23] R.M. De Carlo, L. Rivoira, L. Ciofi, C. Ancillotti, L. Checchini, M. Del Bubba, M.C. Bruzzoniti, Evaluation of
529 different QuEChERS procedures for the recovery of selected drugs and herbicides from soil using LC
530 coupled with UV and pulsed amperometry for their detection, Analytical and Bioanalytical Chemistry 407(4)
531 (2015) 1217-1229. https://doi.org/https://doi.org/10.1007/s00216-014-8339-x.
532 [24] United States of Pharmacopoeia 38 NF 33, United States Pharmacopeial Convention,General chapter
533 <621>, Chromatography, 2015, pp. 424-434.
534 [25] D. Brunel, A.C. Blanc, E. Garrone, B. Onida, M. Rocchia, J.B. Nagy, D.J. Macquarrie, Spectroscopic
535 studies on aminopropyl-containing micelle templated silicas. Comparison of grafted and co-condensation
536 routes, in: R. Aiello, G. Giordano, F. Testa (Eds.), Stud. Surf. Sci. Catal., Elsevier2002, pp. 1395-1402.
537 https://doi.org/https://doi.org/10.1016/S0167-2991(02)80305-6.
538 [26] B. Onida, L. Borello, C. Busco, P. Ugliengo, Y. Goto, S. Inagaki, E. Garrone, The surface of ordered
539 mesoporous benzene - Silica hybrid material: An infrared and ab initio molecular modeling study, J. Phys.
540 Chem. B 109(24) (2005) 11961-11966. https://doi.org/10.1021/jp050686n.
541 [27] Y.Y. Ye M., Trinh A., Analysis of Multi-Pesticide Residues in Vegetables, Food, and Fruits by SPE/GC-MS,
542 available at https://www.sigmaaldrich.com/content/dam/sigma-
543 aldrich/docs/Supelco/Posters/t405020h.pdf last accessed September 2020.
544 [28] O. Shimelis, Y. Yang, K. Stenerson, T. Kaneko, M. Ye, Evaluation of a solid-phase extraction dual-layer
545 carbon/primary secondary amine for clean-up of fatty acid matrix components from food extracts in
546 multiresidue pesticide analysis, J. Chromatogr. A 1165(1) (2007) 18-25.
547 https://doi.org/https://doi.org/10.1016/j.chroma.2007.07.037.
548 [29] F. Plössl, M. Giera, F. Bracher, Multiresidue analytical method using dispersive solid-phase extraction
549 and gas chromatography/ion trap mass spectrometry to determine pharmaceuticals in whole blood, J.
550 Chromatogr. A 1135(1) (2006) 19-26. https://doi.org/https://doi.org/10.1016/j.chroma.2006.09.033.
551 [30] D. Orso, M. Martins, F. Donato, T. Rizzetti, M. Kemmerich, M. Adaime, R. Zanella, Multiresidue
552 Determination of Pesticide Residues in Honey by Modified QuEChERS Method and Gas Chromatography
553 with Electron Capture Detection, Journal of the Brazilian Chemical Society 25 (2014).
554 https://doi.org/10.5935/0103-5053.20140117.
555 [31] C. Ling, X. Li, Z. Zhang, F. Liu, Y. Deng, X. Zhang, A. Li, L. He, B. Xing, High adsorption of
556 sulfamethoxazole by an amine-modified polystyrene–divinylbenzene resin and its mechanistic insight,
557 Environmental science & technology 50(18) (2016) 10015-10023.
558 https://doi.org/https://doi.org/10.1021/acs.est.6b02846.
559 [32] G. Wells, H. Prest, C.W. Russ IV, Why use signal-to-noise as a measure of MS performance when it is
560 often meaningless? , Technical Overview, Agilent Technologies (2011) available at
561 https://www.google.com/url?sa=t&rct=j&q=&esrc=s&source=web&cd=&cad=rja&uact=8&ved=2ahUKEwiN
562 _76uuJPuAhVPCuwKHY_cDTUQFjABegQIBxAC&url=https%3A%2F%2Fwww.agilent.com%2Fcs%2Flibrary%2
563 Ftechnicaloverviews%2Fpublic%2F5990-8341EN.pdf&usg=AOvVaw35pJ2yCwYqtgeugpe9ySZj.
564 [33] J. Bérubé, C. Wu, Signal-to-noise ratio and related measures in parameter design optimization: an
565 overview, Sankhyā: The Indian Journal of Statistics, Series B (2000) 417-432.
566 [34] L. Rivoira, R.M. De Carlo, S. Cavalli, M.C. Bruzzoniti, Simple SPE–HPLC determination of some common
567 drugs and herbicides of environmental concern by pulsed amperometry, Talanta 131 (2015) 205-212.
568 https://doi.org/https://doi.org/10.1016/j.talanta.2014.07.070.
569 [35] L. Renai, F. Tozzi, C.V. Scordo, E. Giordani, M.C. Bruzzoniti, D. Fibbi, L. Mandi, N. Ouazzani, M. Del
570 Bubba, Productivity and nutritional and nutraceutical value of strawberry fruits (Fragaria x ananassa Duch.)
571 cultivated under irrigation with treated wastewaters, J. Sci. Food Agric. in press (2020).
572 https://doi.org/10.1002/jsfa.10737.

573 [36] C. Rivera, R. Rodríguez, Horwitz equation as quality benchmark in ISO/IEC 17025 testing laboratory,
574 Private communication (2014).
575 [37] A. Sadowska-Rociek, M. Surma, E. Cieślik, Comparison of different modifications on QuEChERS sample
576 preparation method for PAHs determination in black, green, red and white tea, Environmental Science and
577 Pollution Research 21(2) (2014) 1326-1338. https://doi.org/10.1007/s11356-013-2022-1.
578 [38] J. Dachs, J.M. Bayona, Large volume preconcentration of dissolved hydrocarbons and polychlorinated
579 biphenyls from seawater. Intercomparison between C18 disks and XAD-2 column, Chemosphere 35(8)
580 (1997) 1669-1679. https://doi.org/https://doi.org/10.1016/S0045-6535(97)00248-8.
581 [39] T. Sato, T. Tsuneda, K. Hirao, A density-functional study on π-aromatic interaction: Benzene dimer and
582 naphthalene dimer, The Journal of chemical physics 123(10) (2005) 104307.
583 https://doi.org/https://doi.org/10.1063/1.2011396.
584 [40] X. Yang, C. Zhang, L. Jiang, Z. Li, Y. Liu, H. Wang, Y. Xing, R.T. Yang, Molecular simulation of
585 naphthalene, phenanthrene, and pyrene adsorption on MCM-41, International journal of molecular
586 sciences 20(3) (2019) 665. https://doi.org/https://doi.org/10.3390/ijms20030665.
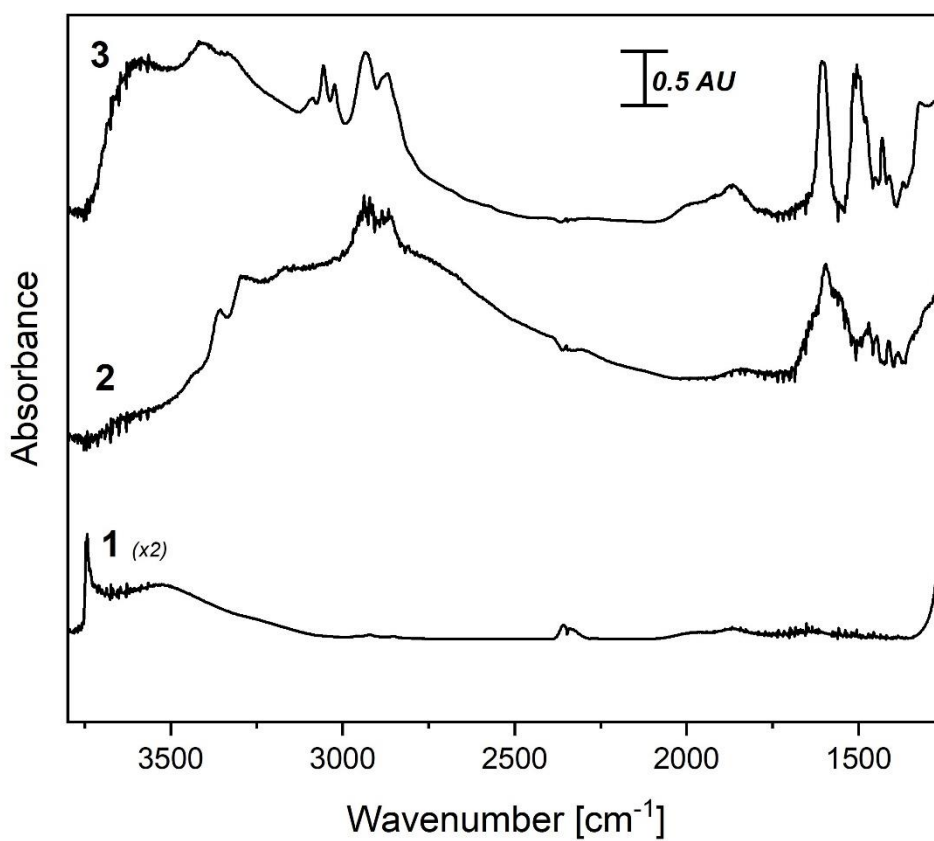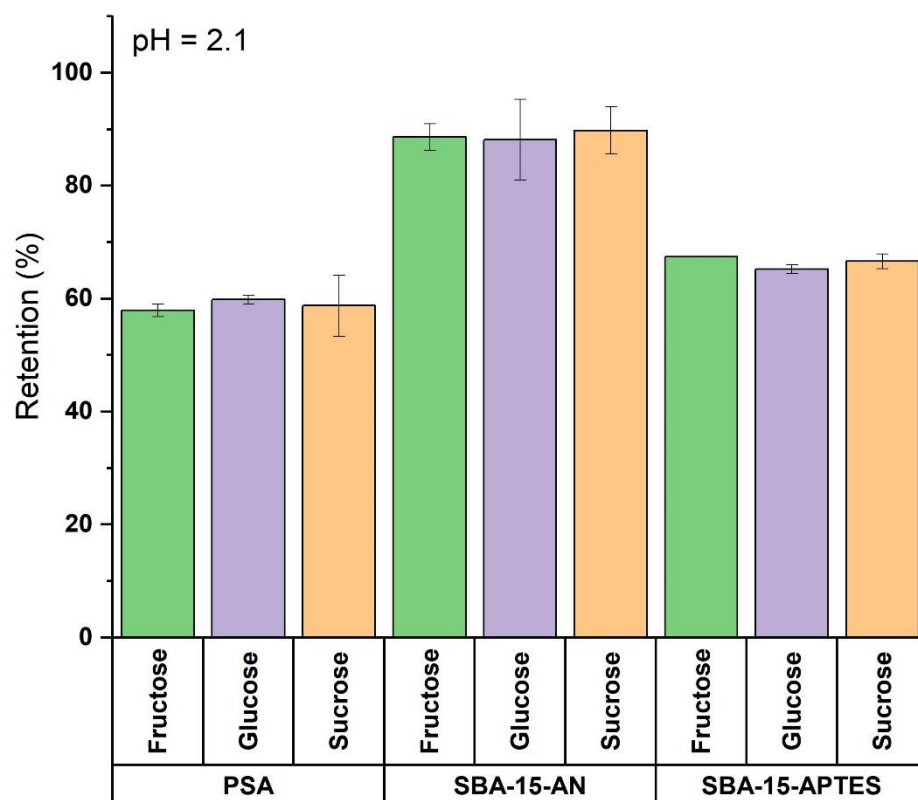587
588

Figure Captions

Fig. 1. Schematic representation of PSA (A) and structure of the precursors APTES (B) and N-[3-(trimethoxysilyl)propyl]aniline (C).
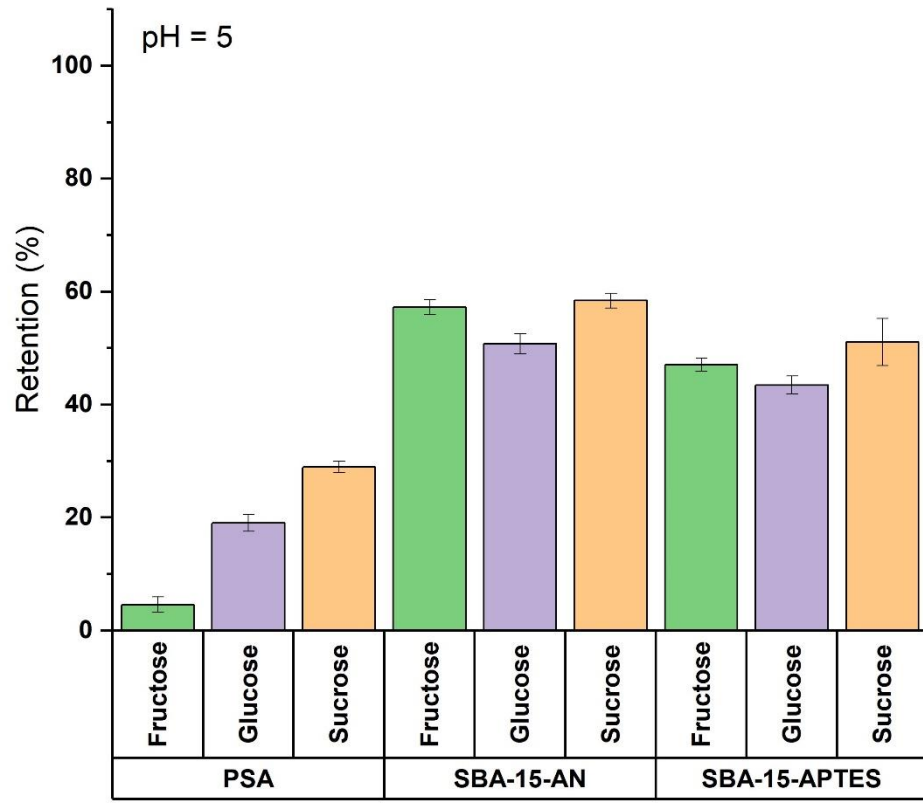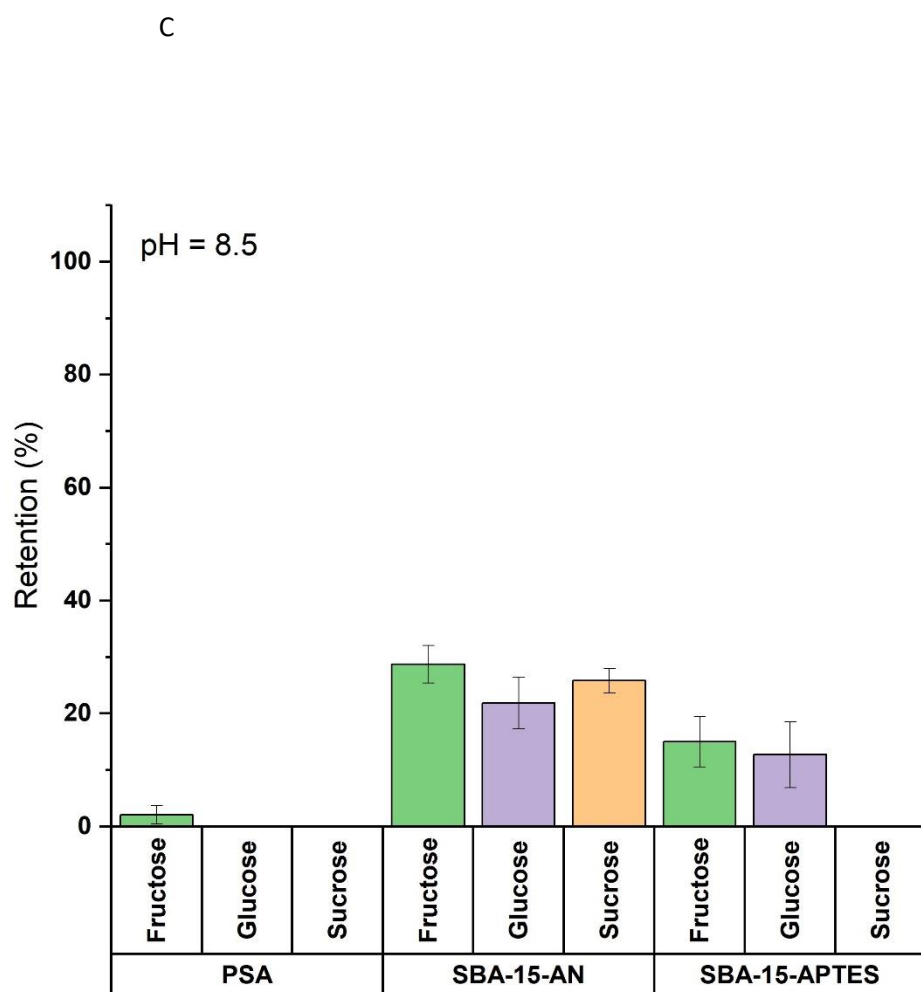
Fig. 2.   FT-IR Spectra of SBA-15 (curve 1), SBA-15-APTES (curve 2) and SBA-15-AN (curve 3). The spectrum of SBA-15 was amplified by a factor 2 for sake of clarity.
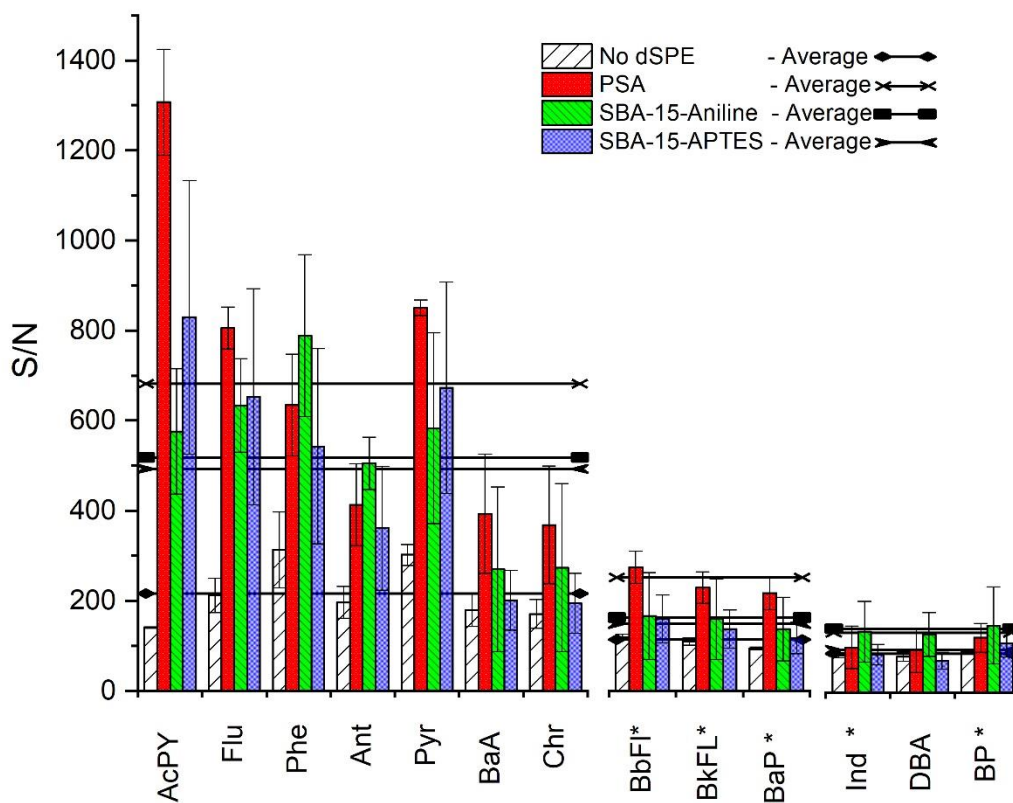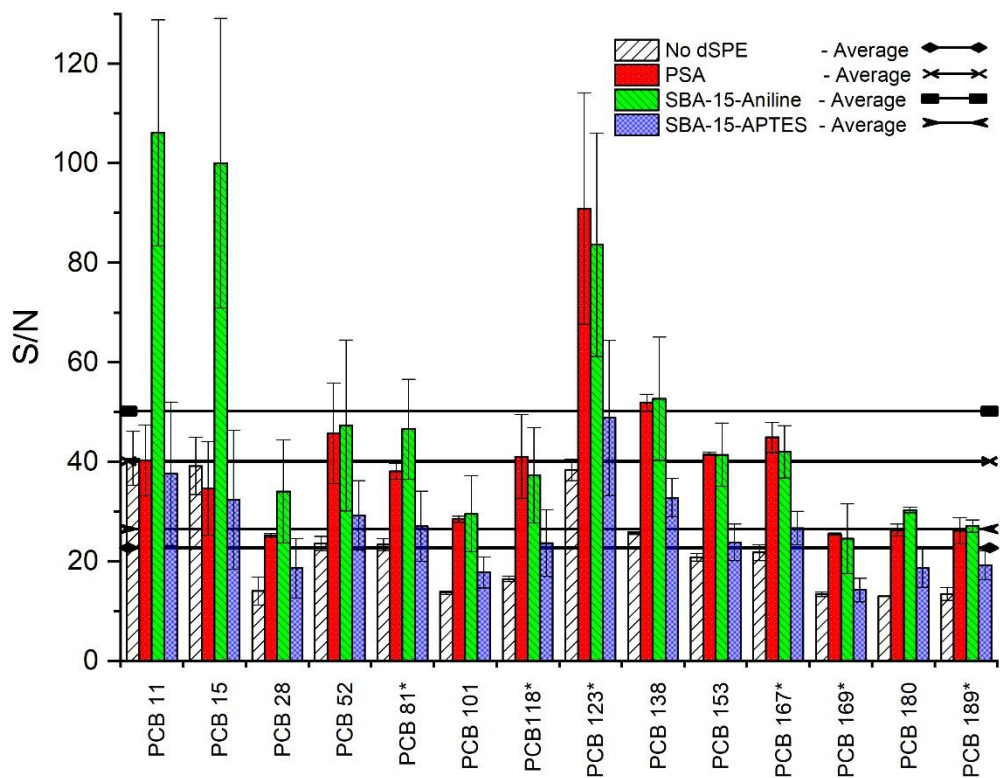
Fig. 3. Adsorption of glucose, fructose, sucrose on PSA, SBA-15-APTES and SBA-15-AN at pH 2.1 (A), 5.0 (B) and 8.5 (C). For experimental details, see text.
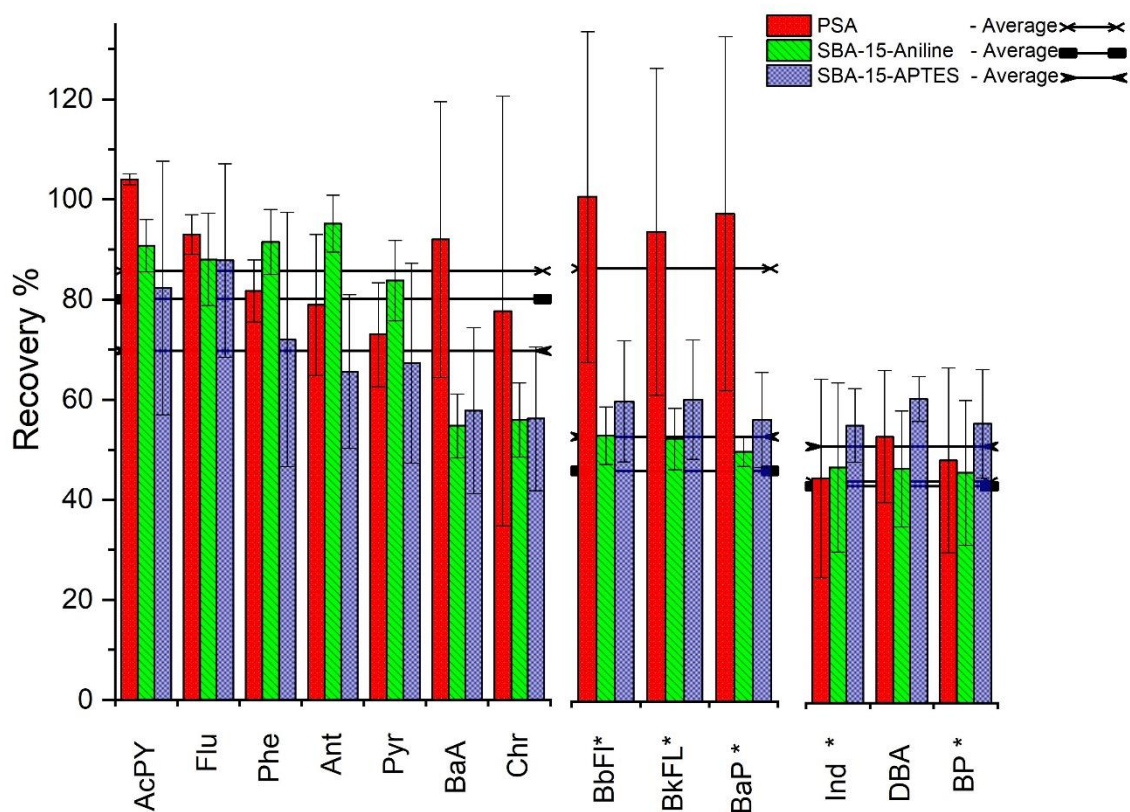
Fig. 4. Signal-to-noise ratio (S/N) obtained after the QuEChERS extraction of PAHs from strawberry, without and with the *d*-SPE clean-up by PSA, SBA-15-APTES and SBA-15-AN. For QuEChERS extraction conditions, see text.

Fig. 5.   Signal-to-noise ratio (S/N) obtained after the QuEChERS extraction of PCBs from strawberry, without and with the *d*-SPE clean-up by PSA, SBA-15-APTES and SBA-15-AN. For QuEChERS extraction conditions, see text.
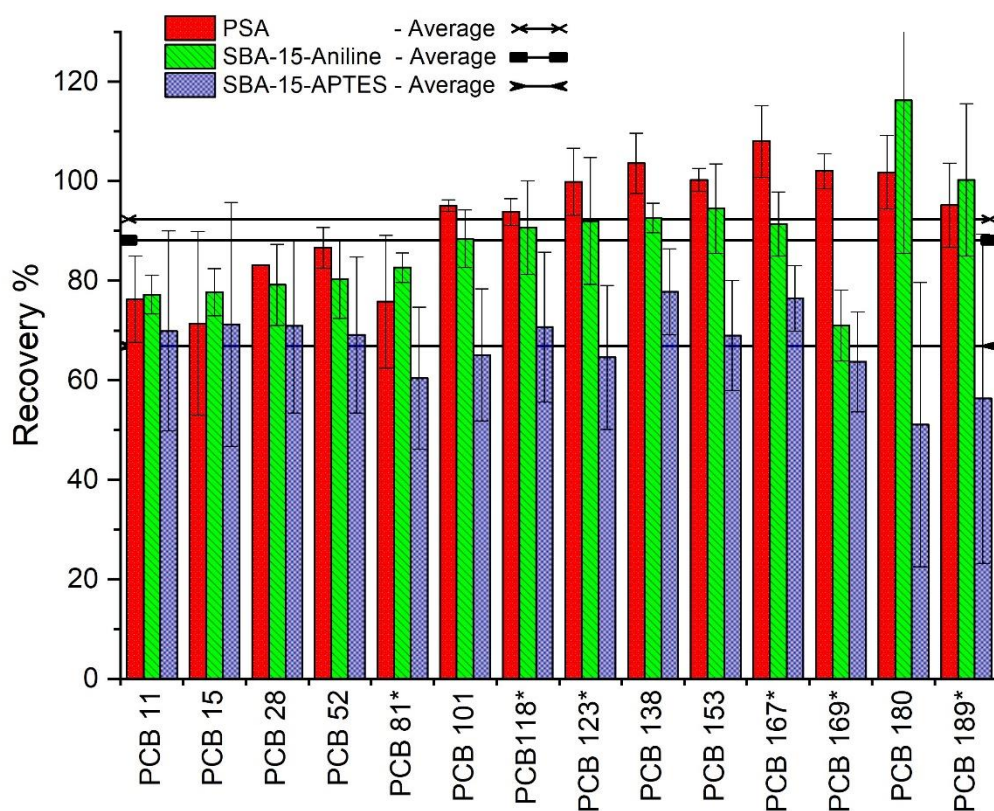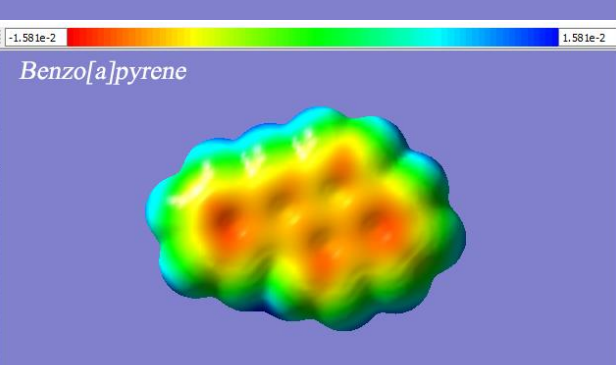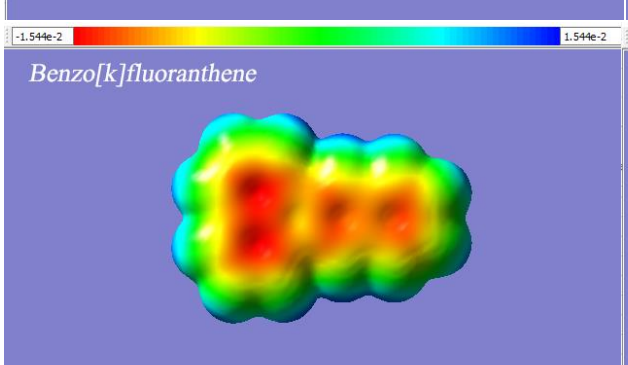
Fig. 6.   Extraction recovery percentage obtained after the QuEChERS extraction of PAHs from strawberry and the *d*-SPE clean-up by PSA, SBA-15-APTES and SBA-15-AN. For QuEChERS extraction conditions, see text.

Fig. 7.   Extraction recovery percentage obtained after the QuEChERS extraction of PCBs from strawberry and the *d*-SPE clean-up by PSA, SBA-15-APTES and SBA-15-AN. For QuEChERS extraction conditions, see text.
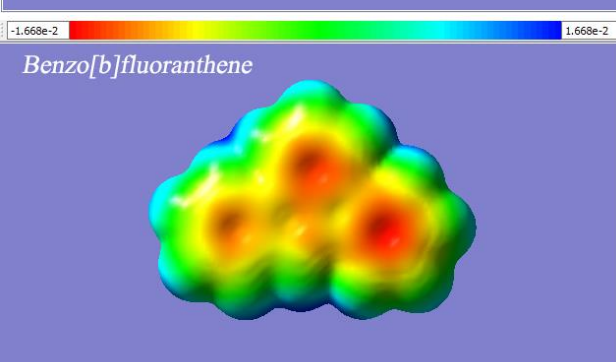
Fig. 8: Electrostatic potential and charge density distribution results of target PAHs, listed following the classes described in paragraph 3.3 (ring classification). At the top of each structure, the colour scale of electrostatic potential distribution (unique for each PAH) is represented, with the blue (red) portion representing the most positive (negative) potential.

Fig. 9. Dependence of PAH (A) and PCB (B) extraction recovery percentage on molecular weight (MW) using SBA-15-AN as *d*-SPE sorbent within the QuEChERS protocol in strawberry.

Fig. 1. Schematic representation of PSA (A) and structure of the precursors APTES (B) and N-[3-(trimethoxysilyl)propyl]aniline (C).

Fig. 2.   FT-IR Spectra of SBA-15 (curve 1), SBA-15-APTES (curve 2) and SBA-15-AN (curve 3). The spectrum of SBA-15 was amplified by a factor 2 for sake of clarity.

A

C

Fig. 3. Adsorption of glucose, fructose, sucrose on PSA, SBA-15-APTES and SBA-15-AN at pH 2.1 (A), 5.0 (B) and 8.5 (C). For experimental details, see text.
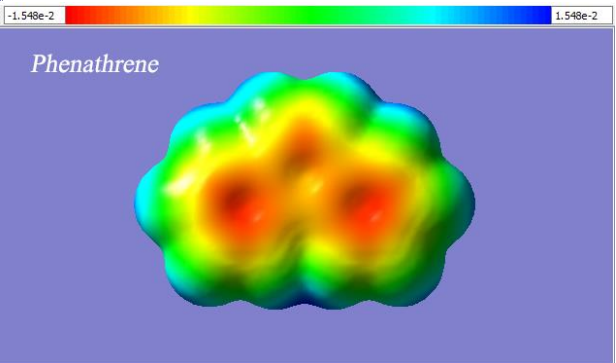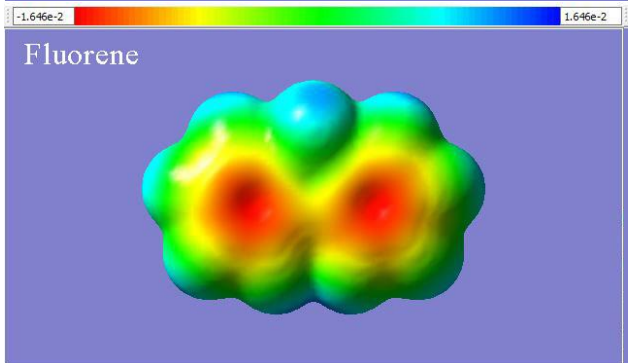
Fig. 4. Signal-to-noise ratio (S/N) obtained after the QuEChERS extraction of PAHs from strawberry, without and with the d-SPE clean-up by PSA, SBA-15-APTES and SBA-15-AN. For QuEChERS extraction conditions, see text
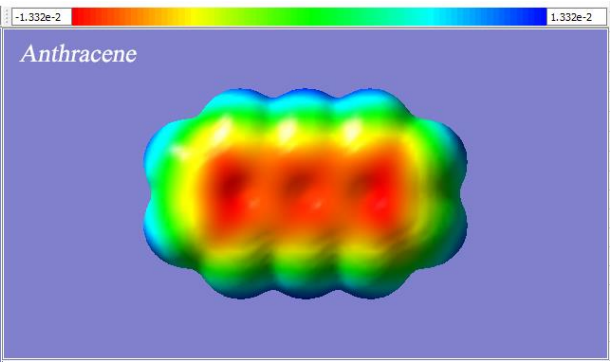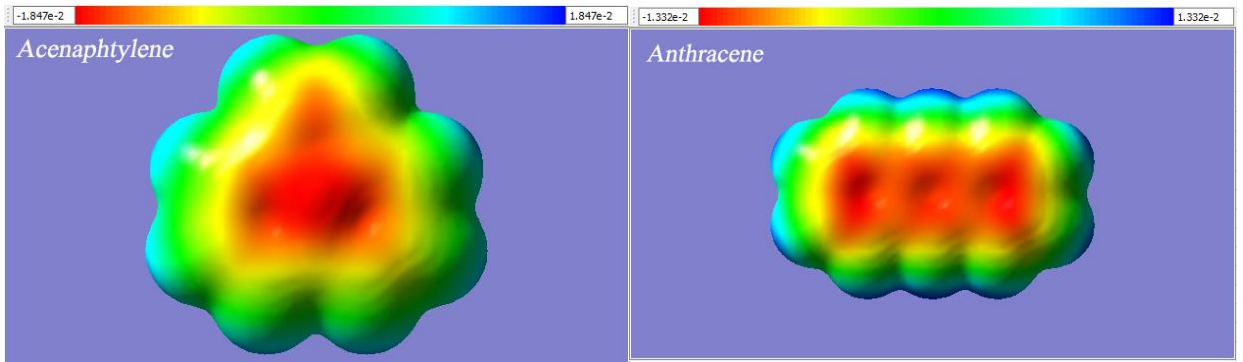
Fig. 5. Signal-to-noise ratio (S/N) obtained after the QuEChERS extraction of PCBs from strawberry, without and with the *d*-SPE clean-up by PSA, SBA-15-APTES and SBA-15-AN. For QuEChERS extraction conditions, see text.
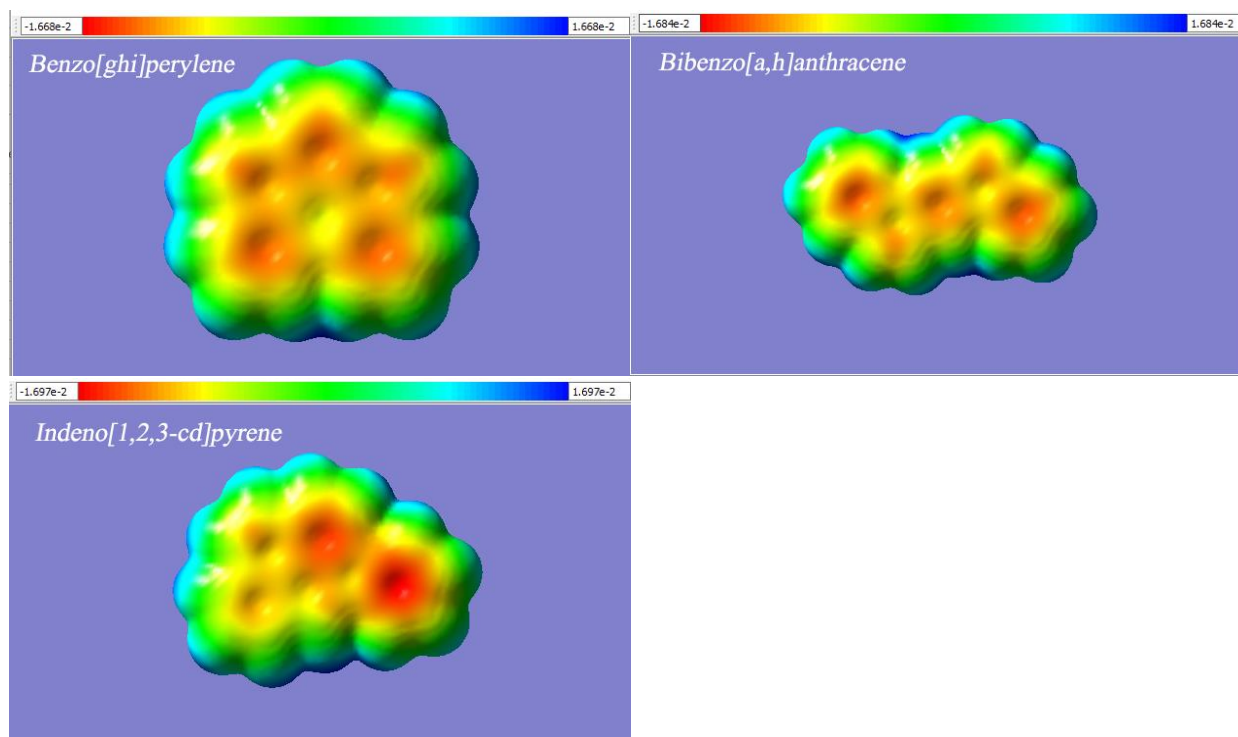
Fig. 6. Extraction recovery percentage obtained after the QuEChERS extraction of PAHs from strawberry and the *d*-SPE clean-up by PSA, SBA-15-APTES and SBA-15-AN. For QuEChERS extraction conditions, see text.
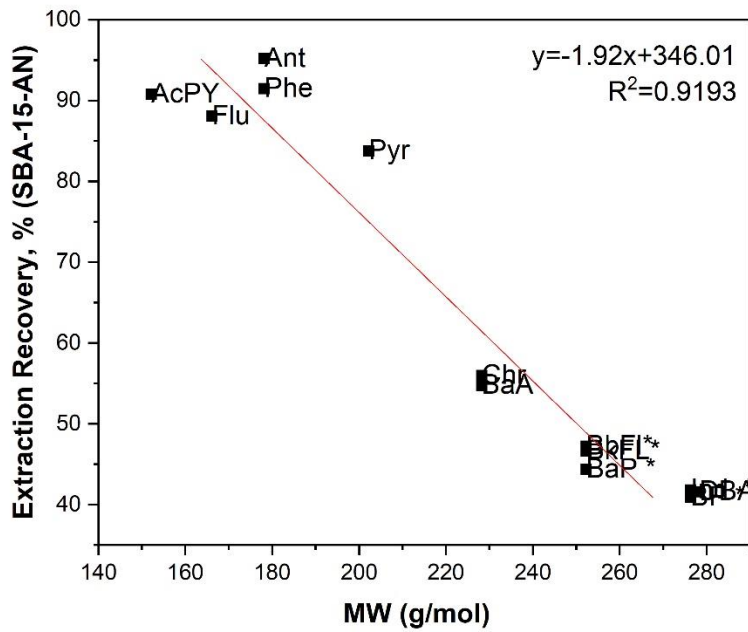
Fig. 7. Extraction recovery percentage obtained after the QuEChERS extraction of PCBs from strawberry and the *d*-SPE clean-up by PSA, SBA-15-APTES and SBA-15-AN. For QuEChERS extraction conditions, see text.
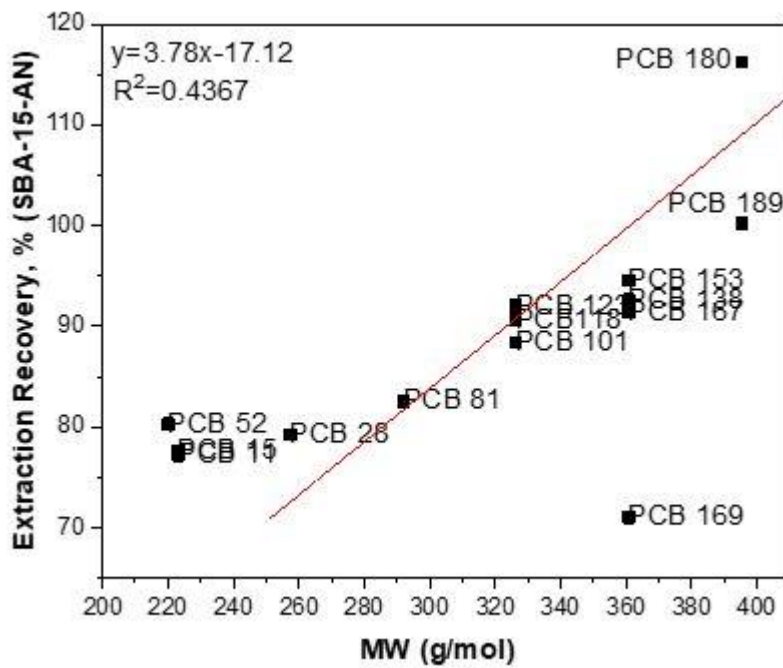
Fig. 8: Electrostatic potential and charge density distribution results of target PAHs, listed following the classes described in paragraph 3.3 (ring classification).

At the top of each structure, the colour scale of electrostatic potential distribution (unique for each PAH) is represented, with the blue (red) portion representing the most positive (negative) potential.

A

B

Fig. 9. Dependence of PAH (A) and PCB (B) extraction recovery percentage on molecular weight (MW) using SBA-15-AN as *d*-SPE sorbent within the QuEChERS protocol in strawberry.

1   **SUPPLEMENTARY INFORMATION SECTION**

2

3   **Amino groups modified SBA-15 for dispersive-solid phase extraction in the analysis of**
4   **micropollutants by QuEChERS approach**

5

6   Michele Castiglioni[a], Barbara Onida[b]*, Luca Rivoira[a], Massimo Del Bubba[c], Silvia Ronchetti[b],
7   Maria Concetta Bruzzoniti[a]*

8

9   [a] Department of Chemistry, University of Turin, Via P. Giuria 7, 10125 Turin, Italy

10   [b] Department of Applied Science and Technology, DISAT, Polytechnic of Turin, Corso Duca degli
11   Abruzzi 24, 10129 Turin, Italy

12   [c] Department of Chemistry "Ugo Schiff", University of Florence, Via della Lastruccia 3, 50019
13   Sesto Fiorentino, Florence, Italy

14

15   ***Corresponding Authors**

16   Prof. Maria Concetta Bruzzoniti

17   ORCID ID 0000-0002-9144-9254

18   Department of Chemistry

19   University of Turin

20   Via P. Giuria 7, 10125 Turin, Italy

21

22   **And**

23

24   Prof. Barbara Onida

25   ORCID ID 0000-0002-1928-3579

26   Department of Applied Science and Technology

27   DISAT, Polytechnic of Turin

28   Corso Duca degli Abruzzi 24, 10129 Turin, Italy

29

Table S1. Main analytical features of the GC-MS method for the determination of PAHs. Chromatographic conditions are detailed in paragraph 2.4 of the main manuscript.

PAHs	Slope	Intercept	R^2	LOD (µg/L)	LOQ (µg/L)
AcPY	1.37	-0.0034	0.9988	0.07	0.22
Flu	1.88	0.0028	0.9984	0.14	0.43
Phe	2.12	0.039	0.9685	0.48	1.46
Ant	0.77	0.003	0.9931	0.15	0.45
Pyr	1.57	0.0076	0.9971	0.13	0.4
BaA	0.91	0.00002	0.9992	0.06	0.18
Chr	1.23	-0.0009	0.9982	0.12	0.35
BbFl	3.7	-0.004	0.9978	0.38	1.15
BkFL	2.76	-0.0041	0.9981	0.27	0.82
BaP	4.12	0.00002	0.9988	0.36	1.07
Ind	5.45	-0.0046	0.9914	1.69	5.12
DBA	4.56	-0.0036	0.9824	2.1	6.36
BP	6.96	-0.0019	0.9976	1.36	4.11

Linearity range: 0.1- 20 µg/L
Intra-day repeatability (n=10): 5.2%
Inter-day repeatability (three days, 10 repetitions for each day, n=30): 9.8%

Table S2. Main analytical features of the GC-MS method for the determination of PCBs. Chromatographic conditions are detailed in paragraph 2.4 of the main manuscript.

PCBs	Slope	Intercept	R^2	LOD (µg/L)	LOQ (µg/L)
PCB 11	4.12	-0.048	0.9982	4.96	14.93
PCB 15	2.62	-0.05	0.9989	2.16	6.55
PCB 28	1.05	-0.026	0.9979	2.99	9.05
PCB 52	1.21	-0.03	0.9982	2.46	7.47
PCB 81	0.87	-0.032	0.9982	1.66	5.04
PCB 101	0.66	-0.014	0.9986	2.03	6.14
PCB 118+123	2.96	-0.064	0.9983	2.87	8.71
PCB 138	1.57	-0.024	0.998	4.31	13.05
PCB 153	0.15	-0.021	0.9981	0.49	1.49
PCB 167	1.23	-0.022	0.9985	2.98	9.04
PCB 169	4.51	-0.046	0.9985	5.4	16.35
PCB 180	0.89	-0.014	0.9981	3.77	11.43
PCB 189	1.07	-0.017	0.9981	4.14	12.54

Linearity range: 1.5- 25 µg/L
Intra-day repeatability (n=10): 4.3%
Inter-day repeatability (three days, 10 repetitions for each day, n=30): 9%